

QUALITY AND STABILITY STUDIES OF THE BEAMS IN THE ELENA RING TRANSFER LINES

J. R. Hunt, O. Karamyshev, J. Resta-López, C. P. Welsch
 Cockcroft Institute and The University of Liverpool, UK

Abstract

The Extra Low Energy Antiproton (ELENA) ring will initially provide eight different experiments at CERN with extra low energy (~100 keV) antiprotons by utilising electron cooling techniques. As a result, a system of transfer lines is being designed to ensure each experiment receives a beam consistent with specified properties. In this paper, particle tracking simulations are performed to explore the effects of different lattice imperfections, e.g. element misalignment, electric field errors and matching errors, on the beam quality and orbit stability. Specific values for the upper limits of inaccuracies are obtained as a guide for the construction of the transfer lines, and will enable further optimization.

INTRODUCTION

ELENA is a low energy storage ring designed to increase the efficiency of the antimatter experiments at CERN [1]. Currently under construction, ELENA will accept antiprotons from the Antiproton Decelerator (AD) [2] and employ the use of an electron cooler to further decelerate them from a kinetic energy of 5.3 MeV to 100 keV. At these lower energies, fewer antiprotons will be lost to degrader foils at the end of the deceleration process and as a result the anti-hydrogen experiments will receive higher intensity beams.

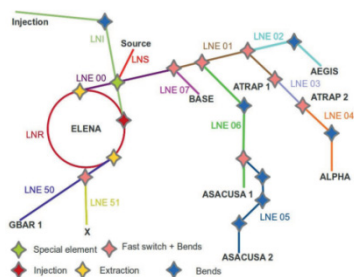


Figure 1: Schematic layout of transfer lines.

A system of transfer lines will carry these extra low energy beams to eight different locations within the AD hall. The low beam energy after ejection from ELENA allows the use of electrostatic elements. Reasons for this design choice include cost of construction, low power consumption, easy operation and good possibilities for shielding elements against stray magnetic fields. [1]

Nine separate lattices make up the transfer lines, two of which are directly connected to ELENA. The studies

Work supported by the EU under Grant Agreement 624854 and the STFC Cockcroft Institute core grant No. ST/G008248/1.
 james.hunt@cockcroft.ac.uk

undertaken in this paper focus on the lattice 'LNE00' as it is connected directly to ELENA and the beams for all but one experiment will pass through this section, see Fig. 1. The only working optical elements present along LNE00 in these simulations are the quadrupoles in a configuration used to pass the beam through to LNE01.

TRACKING CODE

For this study Polymorphic Tracking Code (PTC) [3] was used to track a series of beams through a complete MAD-X [4] model of LNE00 obtained from [5]. For each simulation, a Gaussian beam of 10,000 particles with initial ϵ_x and $\epsilon_y = 1$ mm-mrad, momentum spread = 5×10^{-4} and no x-y coupling, was generated using Monte-Carlo methods. After tracking, the beam data was passed to a custom Matlab code for analysis.

ELEMENT POSITION OFFSETS

The positions of the quadrupoles were offset in the x and y planes separately. Monte-Carlo methods were used to offset each element by a random amount corresponding to a Gaussian spread. The magnitude of the offsets was increased and the effect on the particle losses in the beam was observed (Fig. 2). For each point the result of 10 runs with varying random offsets were averaged to capture overall effect of the position errors.

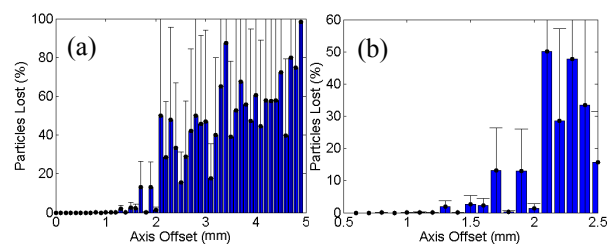


Figure 2: Horizontal losses at the end of LNE00 for increasing quadrupole offsets. The vertical losses results have similar features. (a) shows the full scan and (b) shows more detail around 1.5 mm.

The effects of the quadrupole offsets on the beam losses at the end of the transport line remain steady until they significantly increase around 1.8 mm, with the average reaching just below full beam loss by 5 mm. The first significant losses occur at 1.3 mm where for one particular run almost 18% of the beam was lost, however the other 9 runs lost only 0.56% in total, bringing the average down.

As this simulation only includes the physical aperture and we would expect a dynamic aperture at a smaller

radius we suggest a preliminary maximum position error of 1 mm for the quadrupoles in LNE00. This will decrease when considering other configurations of the optics of the line, particularly when transferring to LNE07 using kickers. It should be noted that for other lines along the transfer system, elements such as kickers and bending magnets will also contribute to particle losses which must be taken into account when performing additional studies across the transport system.

BEAM INJECTION MISMATCH

A good match between the lattice parameters of the extracted beam and the beam transfer lines is essential to minimize particle losses. In this section we explore the effects of a mismatch of the beam which could occur for a variety of reasons, e.g. due to non-optimum voltage or magnet settings and fluctuations in power supplies.

In order to study the effects of a β -function mismatch upon entering the transfer line, three series of 100 beams each with a range of β_x , β_y and momentum spread values were generated separately. The β_x and β_y variations lead to maximum mismatch parameters (B_{mag}) of 2.4821 and 1.1905, respectively. The mismatch parameter was calculated using:

$$B_{mag} = \frac{1}{2} \left[\left(\frac{\beta}{\beta_*} + \frac{\beta_*}{\beta} \right) + \left(\alpha_* \sqrt{\frac{\beta}{\beta_*}} - \alpha \sqrt{\frac{\beta_*}{\beta}} \right)^2 \right], \quad (1)$$

where the * subscripts denote the mismatched lattice parameters [6].

The emittance for each of these beams was calculated and plotted. The effect of the mismatching on the emittance was negligible even beyond values that correspond to a beta mismatch of almost 50%. To further understand the effects of a β -function mismatch the profiles of the beams in phase space were considered (Fig. 3). It can clearly be seen that the β_x -function mismatch has a detrimental effect on the projected beam sizes as we would expect – they increase with increasing B_{mag} . However in the case of a β_y -function mismatch the effect is much less pronounced. This is because although the β values have both been varied by the same percentage amount, the B_{mag} value they correspond to is different due to a dependence on α , α_x is much larger than α_y .

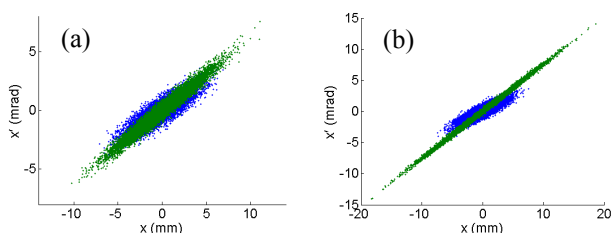


Figure 3: Beams in phase space for (a) $B_{mag} = 1$ (blue) & 1.8 (green) and (b) $B_{mag} = 1$ (blue) & 7 (green) due to a β_x mismatch.

An investigation into particle losses was also carried out with a more significant β mismatch – a pessimistic case of a 200% increase, corresponding to $B_{mag} \approx 7$ for β_x . Particle losses begin to rise steadily from $B_{mag} \approx 3$, and although the errors are large due to a low number of realisations per point, a clear trend can be seen (Fig. 4).

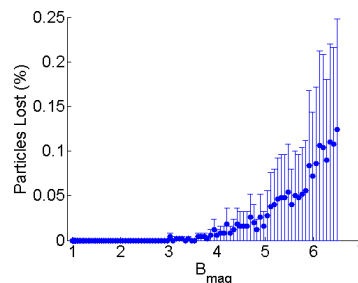


Figure 4: Horizontal losses at the end of LNE00 due to significant β_x mismatching.

QUADRUPOLE FIELD STRENGTH ERRORS

Fluctuations in the field strength of quadrupoles along LNE00 were also simulated. With the Gaussian smearing method used in the element position offsets study, the strengths of each quadrupole were varied independently from each other. This was repeated for 10 random iterations before the strength of the error was increased by 1%.

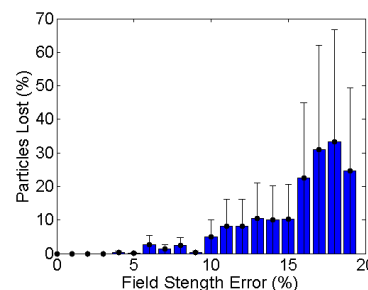


Figure 5: Results of the quadrupole field strength scan along LNE00, the large error bars are due to the random nature of the variations, but a clear overall trend can be seen.

Figure 5 shows the results of the scan along LNE00, the large error bars are due to the random nature of the variations, but a clear overall trend can be seen. Significant particle loss does not occur until a field strength error of around 11%. However, significant particle loss did occur earlier than this for specific runs. This is due to configurations of field error that are by chance more effective at blowing the beam up, for example the first and second elements (LNE.ZQMF.0002 and LNE.ZQMD.0005) have an extremely large error in the same direction. These cases are relatively rare (around one in thirty), but could be explored in future studies,

perhaps to identify particularly error sensitive elements or combinations along the line.

FINITE ELEMENT SIMULATIONS & MULTIPOLAR COMPONENTS

Studies to determine the multipolar components of the electrostatic elements are underway [7]. The finite element program COMSOL Multiphysics was used to create a test quadrupole with the geometry of those used along LNE00 (Fig. 6). For now, arbitrary voltages of ± 500 V were applied to the opposing poles and a cylindrical shaped shield was added 10 mm from the ends of the element.

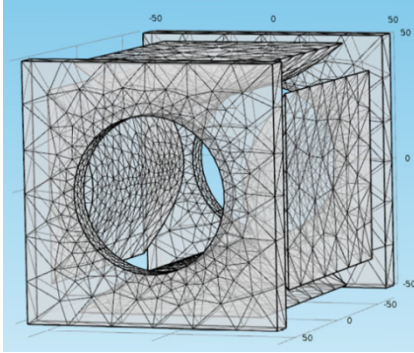


Figure 6: COMSOL Multiphysics model of LNE00 quadrupole with initial mesh.

In order to find the different components of the field, the electric potential around a transverse circle ($\varphi = 0.2\pi$) at fixed z and radius was calculated. The multi-polar components can then be found in a Taylor expansion of the electric potential in cylindrical co-ordinates:

$$V(R, \varphi, z) = \frac{q}{2E_{kin}} \sum \frac{1}{n!} A_n(z) R^n e^{in\varphi}, \quad (2)$$

where A_1 = dipole, A_2 = quadrupole, A_3 = sextupole, A_4 = octupole... components.

Fitting the circular scan of $V(R, \varphi, z)$ with

$$V(R, \varphi, z) = K \cos(2x) + D \cos(6x), \quad (3)$$

gives the quadrupole, K , and dodecapole, D , components of the field. K and D were then calculated along z and the effective overall quadrupole and dodecapole coefficients k_{eff} and d_{eff} were found by using the integrals in Eq. (4).

$$k_{eff} = \int \frac{2qLK(z)}{2E_{kin}R^2} dz \quad d_{eff} = \int \frac{6!qLD(z)}{2E_{kin}R^6} dz. \quad (4)$$

This process was repeated for a model with quadrupole shaped shields, the results are shown in Table 1.

Table 1: Field Co-efficients For Different Electrode Shapes

Shield Shape	$k_{eff} (m^{-1})$	$d_{eff} (m^{-5})$
Cylindrical	0.6018	3.4210×10^6
Quadrupolar	0.6069	1.6354×10^5

Analytically calculating k_{eff} for a hard edge quadrupole using Eq. (5) gives us

$$k_{eff} = \frac{qU_{total}}{2E_{kin}R^2} L = 0.5556 (m^{-1}) \quad (5)$$

This result is in good agreement with those obtained numerically with the finite element methods, within 10%. However, we expect some disagreement as the hard edge model is a simplified case.

These coefficients can be easily implemented to the MAD-X model of the ELENA transfer lines for a continuation of the studies presented in earlier sections.

CONCLUSION AND OUTLOOK

The work presented in this paper represents the first steps in developing a multi-knob simulation platform for carrying out a detailed analysis of the impact from various factors on the resulting beam quality in electrostatic transfer lines. First tests were done for the example of the ELENA beam lines and in particular LNE00 has been studied in its most basic configuration, with no kickers or deflectors enabled. However, the work on the quadrupoles provides a good blueprint for the implementation of additional optical elements, such as kickers and bending elements, along the whole of the transfer system. Furthermore, work to calculate the multipolar components of the quadrupole fields will also be extended to include these additional optical elements.

REFERENCES

- [1] V. Chohan (editor), "Extra Low Energy Antiproton ring" and its Transfer Lines, Design Report," CERN-2014-002 (2014).
- [2] S. Maury (editor), "Design Study of the Antiproton Decelerator: AD," CERN/PS 96-43 (AR), 1996.
- [3] É. Forest et. "Introduction to the Polymorphic Tracking Code," CERN-SL-2002-044 (AP).
- [4] G. Roy (editor), "The MAD-X Program User's Reference Manual", Preliminary Draft: <http://cern.ch/madx/madX/doc/latexuguide/madxuguide.pdf>
- [5] M. Fraser, online directory: http://mfraser.web.cern.ch/mfraser/public/ELENA/MADX/v1_8/
- [6] A. Wu Chao, M. Tigner, *Handbook of Accelerator Physics and Engineering*, (World Scientific, 1999), 253.
- [7] O. Karamyshev et. al "Optimization of Low Energy Electrostatic Beam Lines", TUPRO071, Proceedings of IPAC 2014, Dresden Germany.